Molecular Crystals and Liquid Crystals Science and Technology. Section A. Molecular Crystals and Liquid Crystals

Publication details, including instructions for authors and subscription information:
http://www.tandfonline.com/loi/gmcl19

MORPHOLOGICAL TRANSFORMATIONS DURING PHASE-SEPARATION/ORDERING PHENOMENA

Aleksij Aksimentiev [a]

[a] Material Science Laboratory, Mitsui Chemicals, Inc., 580-32 Nagaura, Sodegaura-City, Chiba, 299-0265, Japan

Version of record first published: 24 Sep 2006

To cite this article: Aleksij Aksimentiev (2001): MORPHOLOGICAL TRANSFORMATIONS DURING PHASE-SEPARATION/ORDERING PHENOMENA, Molecular Crystals and Liquid Crystals Science and Technology. Section A. Molecular Crystals and Liquid Crystals, 366:1, 893-900

To link to this article: http://dx.doi.org/10.1080/10587250108024032

Mol. Cryst. and Liq. Cryst., 2001, Vol. 366, pp. 893-900
Reprints available directly from the publisher
Photocopying permitted by license only

Morphological Transformations During Phase-Separation/Ordering Phenomena

ALEKSIJ AKSIMENTIEV

Material Science Laboratory, Mitsui Chemicals, Inc. 580-32 Nagaura, Sodegaura-City, Chiba 299-0265, Japan

The quantitative analysis of the morphological transformations in asymmetric and symmetric binary mixtures undergoing the phase separation has been reported. The general features of the bicontinuous morphology evolution have been discussed from the standpoint of the dynamic scaling hypothesis. The method for the quantitative characterization of the percolation transition by calculating the Euler characteristic has been described. It has been shown that the transformation of the bicontinuous morphology into droplets involves formation of the transient "cylindric" morphology composed of highly elongated, disconnected droplets.

Keywords: Phase-separation; morphology; percolation

I. INTRODUCTION

Morphology is an ubiquitous feature of any multi-component system: any spatial variation of a local property (for example, concentration) can be viewed as a complex geometrical object by drawing the isosurfaces. Also, any process of the phase separation or ordering can be considered as a time-dependent morphological transformation. For example, if a homogeneous binary mixture (AB) is quenched into the unstable part of its miscibility gap, the domains rich in A or B component will be formed shortly after the quench. In the case of a symmetric mixture, a single bicontinuous interface is formed, Figure 1(left). The domains grow on average with time while their connectivity decreases. In a strongly asymmetric case, the disconnected droplets are formed at the very beginning of the phase-separation process, Figure 1(right). The average domain growth reduces the number of the droplets, their shapes become more and more spherical with time. At some specific quench conditions, the transformation

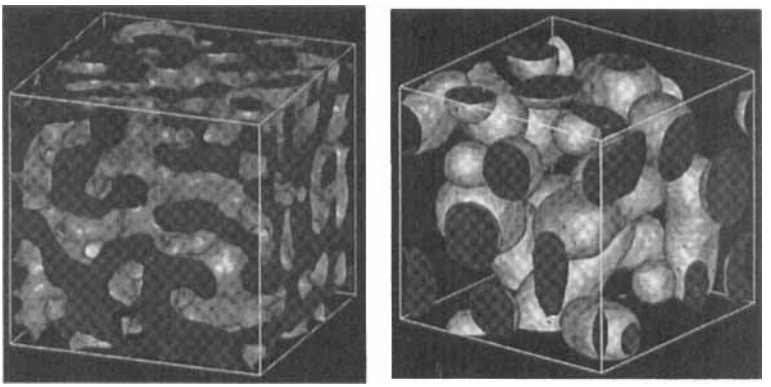

FIGURE 1. Bicontinuous and droplet morphologies.

from bicontinuous to droplet morphology occurs at the intermediate stages of the phase separation. The study of such morphological transformations were hampered in the past by the lack of adequate experimental tools and theoretical methods. The resent advance of the experimental techniques, such as the Laser Scanning Confocal Microscopy (LSCM) [1, 2] and the Transmission Electron Micro-Tomography (TEMT) [3] made possible to visualize directly the interface in the 3D polymer systems, measure the surface area and obtain the curvature distributions.

The obvious advantage of the full morphological description in comparison to the conventional scattering data is in giving the information about the interface topology. A quantity that describes the surface topology is a genus, g, and the Euler characteristic, $\chi_{euler} = 2(1 - g)$. The genus has a very simple interpretation: for a closed surface it is the number of holes in the surface. Thus, a sphere has $g = 0$ ($\chi_{euler} = 2$), a torus $g = 1$ ($\chi_{euler} = 0$, and a pretzel $g = 2$ ($\chi_{euler} = -2$). A large and negative Euler characteristic indicates a highly interconnected, bicontinuous morphology. In contrast, a disconnected droplet morphology is characterized by the large and positive Euler characteristic, because the Euler characteristic of a system of the disconnected surfaces is equal to the sum of the Euler characteristics for the individual surfaces. The computation of the Euler characteristic can be done according to the Euler formula: $\chi_{euler} = F + V - E$ where F, V, E are the number of faces (F), vertices (V), and edges (E) of all polygons cut by the surface in the lattice subunits [4]. Thus, the domain connectivity can be

characterized quantitatively in an ambiguous way, which cannot be done basing on the scattering data or 2D micrographs.

II. GENERAL FEATURES OF THE BICONTINUOUS MORPHOLOGY EVOLUTION

The systems undergoing phase transitions (like spinodal decomposition) often exhibit scaling phenomena [5], i.e. a morphological pattern of the domains at earlier times looks statistically similar to a pattern at later times apart from the global change of scale implied by the growth of $L(t)$ – the domain size. Quantitatively it means for example that the correlation function of the order parameter (density, concentration, magnetization etc.)

$$g(\mathbf{r},t) = g(\mathbf{r}/L(t)), \tag{1}$$

where

$$L(t) \sim t^n, \tag{2}$$

the characteristic length scale in the system, scales algebraically with time t with the exponent n different for different universality classes [5]. The Fourier transform of the correlation function gives the scattering intensity which can be represented by the following scaling form:

$$S(q,t) = L^d(t)Y(qL(t)), \tag{3}$$

where q is the scattering wave-vector and Y is the scaling function. Assuming the scaling hypothesis we can derive all the scaling laws for different morphological measures such as: the Euler characteristic, $\chi(t)$, , surface area, $S(t)$, the distribution of the mean, $P(H,t)$, and Gaussian, $P(K,t)$, curvatures. The scaling hypothesis implies the following scaling laws for any phase separating/ordering symmetric system irrespective of the universality class

$$\chi(t) \sim L(t)^{-3}, \tag{4}$$

$$S(t) \sim L(t)^{-1}, \tag{5}$$

$$P_H(H,t) \sim P_H^*(HL(t))/L(t), \tag{6}$$

$$P_K(K,t) \sim P_K^*(KL(t)^2)/L(t)^2. \tag{7}$$

The first law follows from the Gauss-Bonnet theorem,

$$\chi = \frac{1}{2\pi}\int dSK \tag{8}$$

relating the Gaussian curvature and the Euler characteristic. Because $K = 1/R_1R_2$, therefore scaling implies $K \sim L(t)^{-2}$. Moreover and in the symmetric system the volume of one of the phases, $V \sim S(t)L(t)$ is fixed therefore $S(t) \sim 1/L(t)$ and the scaling (4) follows. These tests are robust i.e. apply to any symmetric system exhibiting phase ordering/separating kinetics. The exponent n for the algebraic growth of $L(t)$ determines the behavior of all other quantities.

The scaling relations (1)-(7) have been tested in the computer simulations. The following Cahn-Hilliard-Cook equation

$$\frac{\partial\phi(\mathbf{x},\tau)}{\partial\tau} = \frac{1}{2\phi_0(1-\phi_0)}\nabla\left\{\phi(1-\phi)\nabla\left[\frac{\chi_{cr}}{2(\chi-\chi_{sp})}\right.\right.$$
$$\times\ln\frac{\phi}{1-\phi} - \frac{2\chi\phi}{(\chi-\chi_{sp})} - \frac{1}{18\phi(1-\phi)}\nabla^2\phi +$$
$$\left.\left.\frac{1-2\phi}{36\phi^2(1-\phi)^2}(\nabla\phi)^2\right]\right\} + \sqrt{\epsilon}\,\zeta(\mathbf{x},\tau), \qquad (9)$$

has been solved numerically, where the noise term $\zeta(\mathbf{x},\tau)$ has been generated in accordance with the fluctuation-dissipation theorem

$$\langle\zeta(\mathbf{x},\tau)\zeta(\mathbf{x}',\tau')\rangle = -\frac{1}{\phi_0(1-\phi_0)}\nabla\phi(1-\phi)\nabla\delta(\mathbf{x}-\mathbf{x}')$$
$$\times\delta(\tau-\tau'). \qquad (10)$$

and with the noise intensity $\epsilon = \sqrt{(\chi-\chi_{sp})}$. In equations (9) and (10) $\phi(\mathbf{x})$ is the local volume fraction of the component A (ϕ_0 is its average value); χ is the Flory-Huggins interaction parameter, $\chi_{sp} = 1/(2N\phi_0(1-\phi_0))$ and $\chi_{cr} = 2/N$ are the values of χ at the spinodal and the critical point. It has been found that the scaling relations (1)-(5) holds at the late stages of the spinodal decomposition [4]. However, the scaling of local curvature distributions is largely affected by the thermal undulations of the interface induced by the noise term [4]. The local curvature scaling is observed only if the thermal motions of the interface have been smoothen out. Thus, during the measurement by using the LSCM, the thermal undulation are averaged out during the measurement time; in addition, the characteristic size of the thermal undulation is usually smaller than the microscope resolution. Therefore the scaling (6),(7) can be experimentally observed [6].

III. PERCOLATION TRANSITION AND THE EULER CHARACTERISTIC

Possibility of the droplet formation during the spinodal decomposition of a binary mixture depends on two factors: the average blend composition ϕ_0 and the quench depth. It is convenient to regard the transformation from interconnected to disperse morphology as a percolation transition. One assumes that the transformation can be described by considering only geometrical features of the system, particularly studying the minority domain volume fraction f_m. At some special value of f_m (at the percolation threshold value) the morphological transition occurs. It is important to distinguish the average A-component volume fraction (composition), ϕ_0, and f_m. The former quantity is a constant, while f_m can change during the simulations. In the very long time limit f_m approaches its equilibrium value

$$f_m^{eq} = (\phi_0 - \phi_A^{(1)})/(1 - 2\phi_A^{(1)}), \tag{11}$$

where $\phi_A^{(1)}$ is the equilibrium volume fraction of the A component in the minority phase (due to the symmetry of the phase diagram only blend of $\phi_0 \leq 0.5$ are considered). The percolation assumption can be tested by calculating both the Euler characteristics and the minority domain volume fraction. Since the Euler characteristic is the direct measure of the domain connectivity, we identify the domain percolation at the point where the Euler characteristic attains zero value.

In Figure 2 we plot the minority phase volume fraction, f_m, versus the Euler characteristic density for large number of simulation runs performed at different quench condition. For the symmetric blends ($\phi_0 = 0.5$) $f_m = 0.5$ and is independent of time and χ_{euler}/V. For the asymmetric blends, f_m decreases with time and χ_{euler}/V may change the sign. The bicontinuous morphology has not been observed for $f_m < 0.29$ neither the droplet morphology for $f_m > 0.31$. This observation suggests that the percolation occurs at $f_m = 0.3 \pm 0.01$ and the percolation threshold is not very sensitive to the quench conditions.

Thus, one could expect to find a droplet morphology at that quench conditions at which the equilibrium minority phase volume fraction (determined by the lever rule from the phase diagram) is lower than the percolation threshold. However, the time interval

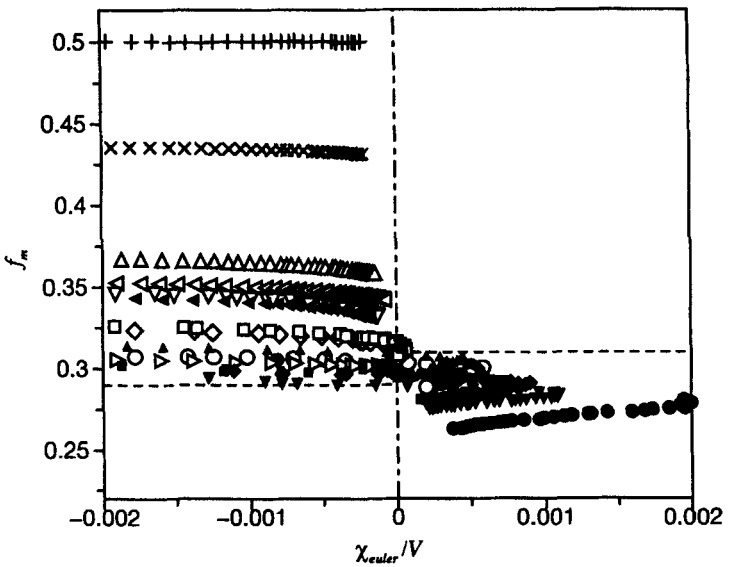

FIGURE 2. The Euler characteristic of the interface as a function of the minority phase volume fraction for different quench conditions.

after which a disperse coarsening occurs would depend strongly on the quench conditions, because the volume fraction of the minority phase approaches the equilibrium value very slowly at the late times.

IV. UNIVERSAL CHARACTER OF THE BICONTINUOUS-TO-DROPLETS TRANSFORMATION

The transformation of the bicontinuous morphology into the disperse droplet pattern is observed in many mesoscopic systems. For example, in the asymmetric diblock copolymer melt the interconnected structures such as a double gyroid phase can be transformed into the disperse spherical morphology (of the BCC or CPS symmetries) by increasing the temperature. The pathway of such transformation involves formation of the cylindrical morphology at the intermediate stage [7]. Similarly, the sponge phase in the surfactant solutions transforms into the micelle phase via some cylindrical mesophases [8]. During the phase separation process, the morphology of the asymmetric binary mixture could be either bicontinuous or disperse,

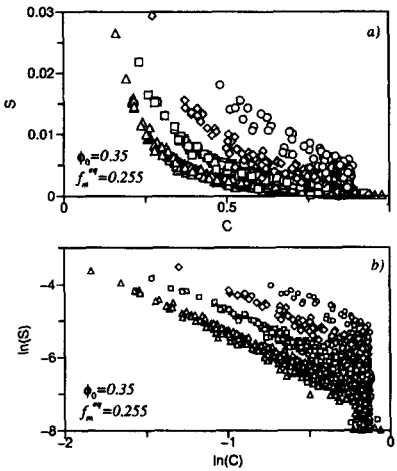

FIGURE 3 Droplet area as a function of its compactness at four time steps.

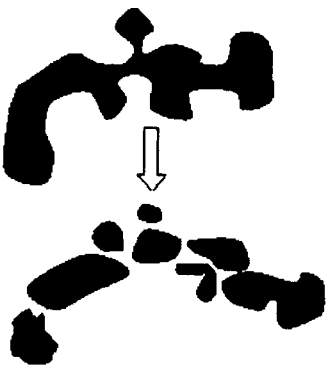

FIGURE 4 Decomposition of a cylindrical droplet.

and, at some quench conditions (when the final equilibrium minority phase volume fraction is slightly below the percolation threshold), this transformation takes place dynamically. The pathway of such transformations can be investigated by analyzing the domain sizes and shapes in a vicinity of the percolation transition $\chi_{Euler} \approx 0$.

In order to find correlations between the shapes and sizes of the domains, the droplet surface area density, S, has been plotted as a function of droplet compactness, C, for each droplet detected in the system at four time steps of the simulation, Figure 3(a). The droplets which have low compactness have sizes bigger than average. When the transformation from bicontinuous to disperse morphology is slow, the power law dependences between the droplet size and compactness can be observed in the low compactness limit. A double-logarithmic plot of these dependences, Figure 3(b), reveals that they are parabolic (the slopes in the low compactness limit are $-2. \pm 0.1$). Consider now a cylindrical (highly elongated) domain of length l and cross section radius R, Figure 4. The area of such a domain is $S \approx 2\pi Rl$, and its compactness $C \approx \frac{3}{\sqrt{2}}\sqrt{R/l}$. Now, if we keep the cross section radius R constant and increase the length of the domain l, the domain area would increase as its compactness

decreases: $S(l) \sim C(l)^{-2}$. That is exactly what is being shown in Figure 3: the droplets are formed due to the decomposition of the highly elongated (cylindrical) domains (see also Figure 4). Thus, also during the phase separation, the transformation from bicontinuous to droplet pattern involves formation of the cylindrical domains, which suggests that it is an universal feature of such transformations.

V. CONCLUDING REMARKS

The results presented above are restricted to the class of binary systems well described by the simple Landau-Ginzburg or Flory-Huggins free-energies. In more complex systems, some morphological features could be significantly different (for example, the percolation threshold value). However, the methods used here to characterize the morphological transformations are not limited to any specific class of the systems and can be used to study any other dynamic or equilibrium phenomena. We hope that this paper will stimulate applications of the quantitative morphological methods in the area of the molecular and liquid crystals.

References

[1] H. Verhoogt, J. van Dam, A. Posthuma de Boer, A. Draaijer, P.M. Houpt, *Polymer*, **34**, 1325 (1993).
[2] H. Jinnai, T. Koga, Y. Nishikawa, T. Hashimoto, S.T. Hyde, *Phys. Rev. Lett.* **78**, 2248 (1997).
[3] H. Jinnai et al, *Phys. Rev. Lett.* **84**, 518 (2000).
[4] A. Aksimentiev, K. Moorthi, R. Holyst, *J. Chem. Phys.* **112**, 6049 (2000).
[5] A.J. Bray, *Adv. in Physics*, **43**, 357 (1994).
[6] H. Jinnai, Y. Nishikawa, T. Hashimoto, *Phys. Rev. E* **59**, R2554 (1999).
[7] K. Kimishima, T. Koga, T. Hashimoto, *Macromolecules*, **33**, 968 (2000).
[8] T. Tlusty, S.A. Safran, R. Strey, *Phys. Rev. Lett*, **84**, 1244 (2000).